

ChartEye: A Deep Learning Framework for Chart Information Extraction

Osama Mustafa

Center of Excellence in AI

Bahria University

Islamabad, Pakistan

muhammadosama939@gmail.com

Muhammad Khizer Ali

Center of Excellence in AI

Bahria University

Islamabad, Pakistan

mkhizer.buic@bahria.edu.pk

Momina Moetesum

School of Electrical Engineering and Computer Science

National University of Sciences and Technology (NUST)

Islamabad, Pakistan

momina.moetesum@seecs.edu.pk

Imran Siddiqi

Xynoptik Pty Limited

Melborne, VIC, Australia

imran.siddiqi@xynoptik.com.au

Abstract—The widespread use of charts and infographics as a means of data visualization in various domains has inspired recent research in automated chart understanding. However, information extraction from chart images is a complex multi-tasking process due to style variations and, as a consequence, it is challenging to design an end-to-end system. In this study, we propose a deep learning-based framework that provides a solution for key steps in the chart information extraction pipeline. The proposed framework utilizes hierarchical vision transformers for the tasks of chart-type and text-role classification, while YOLOv7 for text detection. The detected text is then enhanced using Super Resolution Generative Adversarial Networks to improve the recognition output of the OCR. Experimental results on a benchmark dataset show that our proposed framework achieves excellent performance at every stage with F1-scores of 0.97 for chart-type classification, 0.91 for text-role classification, and a mean Average Precision of 0.95 for text detection.

Index Terms—Chart Infographics, Text-Role Classification, Document AI, Chart-Text Recognition, Object Detection, Text Recognition

I. INTRODUCTION

Data visualization in the form of infographics such as charts, graphs, and plots has been widely adopted for summarization and analytical purposes in various domains. Charts also play a vital role as an integrated component of interactive visualization dashboards due to effective and efficient interpretation of complex data patterns. With the increased use of charts and plots, the need for information extraction from these has also gained popularity. Automatic information extraction from chart images is an emerging area of research that seeks to develop computer vision and natural language processing (NLP) algorithms to identify and extract data points from visual charts such as bar graphs, line plots, and pie charts and interpret their semantics. Primarily two types of information can be extracted from charts i.e. explicit and implicit. Explicit information includes the graphical and textual components that constitute a chart, while implicit information determines their relation with each other and their semantics. Explicit

information extraction is the pre-requisite for implicit understanding and is the prime focus of this research as well. Due to the complexity of the problem, it is divided into several sub-modules or tasks [1]–[3]. The first task involves the identification of the chart type since the information layout of each type is different and may require separate processing. The second step is to detect and recognize the text and graphic components of the chart. This step is vital to determine the semantics of the chart. Another important step is the text-role classification task which identifies the labels and values of the various types of textual information present. For instance, X-axis, Y-axis, legend, titles, etc. The final step is to determine the association between the identified text roles and their values. All these tasks are characterized by challenges like variations in component position, layout, structure, text size, font, and orientation. Figure 1 illustrates some of the chart images to highlight the complexity of the problem. Incorrect extraction of explicit information can adversely impact the implicit inference of chart images.

Due to the challenging nature of the problem, information extraction from chart images has remained an active area of research for the document analysis and recognition (DAR) community. It has also been a regular challenge at popular DAR events like ICDAR 2019 [1], ICPR 2020 [2], and ICPR 2022 [3]. In earlier studies [8], traditional statistical methods (i.e. area, mean, median, and variance) were employed to classify various chart types. High level shape descriptors like Hough transform and histograms of oriented gradients (HOG) were also used for similar purposes by authors in [9]–[11]. These hand-crafted features were then used to train machine learning models like Hidden Markov Model [12], Multiple Instance Learning [13], Support Vector Machines (SVM) [14], [15], and decision trees [16] to identify the input chart type. The main limitation of this approach was the lack of generalization across various types of charts. With the paradigm shift towards deep representation learning, studies like [17]–[20] utilized various deep learning models

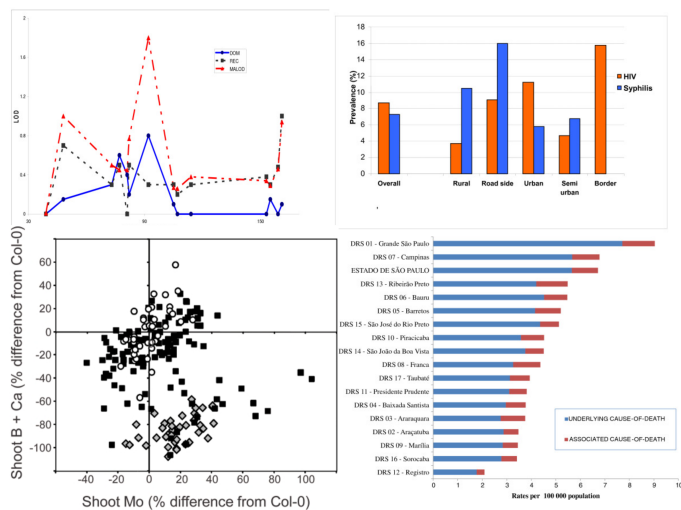


Fig. 1. (a) Line Plot [4] (b) Vertical Bar Chart [5] (c) Scatter Plot [6] (d) Horizontal Bar Chart [7]

like deep belief networks (DBN) and convolutional neural networks (CNN) for the classification of different chart types. Most of these reported near perfect accuracies on basic chart categories like vertical and horizontal bar charts, however, their performance degraded as the number of charts increased.

For the text detection task, most of the earlier studies [15], [21] employed traditional text detection techniques based on connected component analysis to locate textual components in chart images. Geometric (e.g. aspect ratio, width, height), structural (e.g. pixel density, edge orientation), and textural features were also used to identify the location of text in a chart image [12]. However, more recent studies adopted the deep object detection mechanisms for this purpose to enhance performance. For instance, authors in [20], [22], [23] utilized localization methods based on CNNs for chart text detection. Two-stage deep convolutional object detectors like RCNNs have also been employed by studies like [24]–[27]. This was a predominant trend observed in the recent competition submissions of ICPR 2020 and 2021, where most of the teams trained an RCNN variant to accomplish this task. However, most two-stage object detectors are characterized by higher time complexities as compared to one-stage architectures like YOLO. Off-the-shelf commercial tools like Tesseract OCR have also been used for text detection and recognition in chart images [15], [21], [28]. Nonetheless, due to low resolution and small text fonts, the error rate is relatively high [20]. Recently, attention-based mechanisms have been evaluated for chart text detection and recognition [3] and have shown promising results. However, their potential in this domain needs further exploration.

Once detected, the text needs to be categorized based on its role (e.g. legend, axis, value etc.) in the chart. This is a challenging task and requires the extraction of positional

information. Wenjing DaI et al. [20] trained an SVM using positional features for this purpose. A similar technique was proposed by Rabah et al. in [29] using random forest. Xiaoyi et al. [25] utilized a relational network (RN) for role classification in bar charts. Recently, an ensemble-based methodology was described in [2] that combined the output of three models trained on visual, positional, and semantic features. An accuracy of 86% was reported. Wang et al. [30] utilized LayoutLM [31] for this purpose, however, the performance suffered on roles like legend title, legend label, and data markers. Mask RCNN was also evaluated and reported an accuracy of 81.7%. Luo et al. [32] extracted the positional features to train random forest and LightGBM for text-role classification and reported an accuracy of 77%. Recently [3], an RCNN with Swin transformer as backbone was also evaluated on this task and outperformed the state-of-the-art, thus validating the potential of transformers in this domain.

In this study, we propose a deep learning framework for explicit chart information extraction that provides a solution for each of the main steps discussed earlier i.e. chart-type classification, text detection and recognition, and text-role classification. The proposed framework introduces supplementary steps like text resolution enhancement to improve the performance of text recognition that subsequently improves the performance of the next tasks. Our proposed framework can be utilized to extract information from multiple chart-type images, thus providing a generic solution for a number of chart types. Empirical evaluations show that the proposed framework can effectively process digital images of graphical representations and output structured numerical data for further analysis. The main contributions of this study can be summarized as follows:

- A generic pipeline for information extraction from multiple chart-type images based on deep learning techniques.
- Evaluation of the potential of latest attention-based mechanisms for chart-type classification, text recognition and text-role classification tasks.
- Integration of text resolution enhancement step for improved text recognition.

The rest of the paper is organized as follows. Section II describes the proposed methodology in detail. Section III outlines the experimentation protocol. Section IV analyzes the results and finally, Section V concludes the paper.

II. METHODOLOGY

In this section, we discuss the proposed framework in detail. Figure 2 illustrates the main steps in the pipeline i.e. chart-type classification, text detection, detected-text up-scaling, text recognition, and text-role classification. The framework utilizes a combination of deep convolutional and vision transformer-based approaches to effectively extract information from chart images. For instance, for tasks such as text detection, a one-stage object detector is employed, while for chart-type classification and text-role classification, a hierarchical vision transformer is used. In order to enhance the text, an enhanced super-resolution generative adversarial

network (ESRGAN) is utilized. We further explain the low-level architectural details of each sub-task in the subsequent sub-sections.

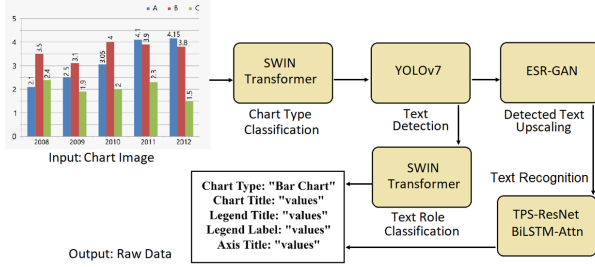


Fig. 2. System pipeline: A diagram illustrating how an input image is processed through different steps of the framework in a pipeline.

A. Chart-Type Classification

Classification of chart type is a challenging task for any classifier, as different charts have increasingly different structures and semantics. Although convolutional neural networks have shown considerable success however, there is still room for improvement in terms of performance and generalization [1]. In our case, we employed the state-of-the-art Swin transformer architecture [33], pre-trained on ImageNet. It is a hierarchical vision transformer that uses shifted windows to generate hierarchical feature maps. Due to contextual learning, it is more robust in the classification of chart types i.e. 15 in our case as shown in Table II. Figure 3 displays high-level architecture of Swin transformer pipeline. An input image is passed through a patch partitioning layer, the output of which enters stage 1 where a linear embedding layer and two Swin blocks are present. In stage 2, patch merging is performed and the output is passed onto the next two Swin blocks. In stage 3, patch merging with six Swin blocks is done. Finally, patch merging with two Swin blocks is repeated. A Swin

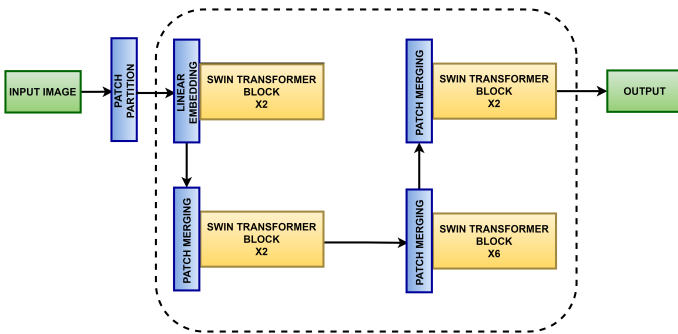


Fig. 3. High-Level architecture of Swin transformer

transformer block consists of a shifted window-based multi-head self-attention MSA (SW-MSA) module, followed by a multi-layered perceptron (MLP), with GELU non-linearity in between. Layer normalization (LN) is applied before each MSA module and each MLP. A skip connection is applied after each module. A detailed architecture of two Swin transformer

blocks is illustrated in the Figure 4. With the shifted window partitioning approach, consecutive Swin transformer blocks are computed as shown in Equations 1, 2, 3, 4.

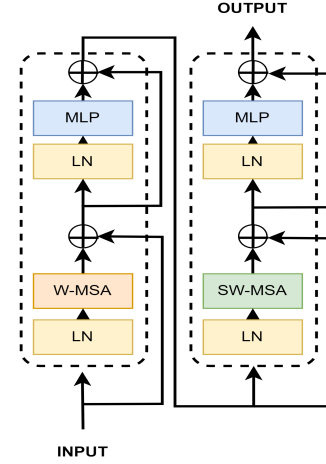


Fig. 4. Architecture of two successive Swin transformer blocks. Multi-headed self-attention modules having regular and shifted windowing configuration are used i.e W-MSA and SW-MSA

$$\hat{z}^l = W - MSA(LN(z^{l-1})) + z^{l-1} \quad (1)$$

$$z^l = MLP(LN(\hat{z}^l)) + \hat{z}^l \quad (2)$$

$$\hat{z}^{l+1} = SW - MSA(LN(z^l)) + z^l \quad (3)$$

$$z^{l+1} = MLP(LN(\hat{z}^{l+1})) + \hat{z}^{l+1} \quad (4)$$

W-MSA and SW-MSA denote window-based multi-head self-attention using regular and shifted window partitioning configurations, respectively. \hat{z}^l and z^l denote the output features of the SW-MSA module and the MLP module for block l , respectively.

B. Text Detection

Text detection is performed on the chart image, focused on logical blocks with a single role. This means that a multi-line axis-title should be detected as a single block. This step performs dual role as it not only detects text for the purpose of recognition but the detected text from this step is also passed on to the last step in pipeline for text-role classification. All types of text such as axis title, legend text, chart title, and tick values are detected. It is a challenging task where there is sometimes increasingly small-scale text present in the image. We performed transfer learning using a state-of-the-art YOLOv7 [34] pre-trained on MS-COCO. It is a single-stage detector that performs object detection by first separating the image into N grids of equal size. Each of these regions is used to detect and localize any objects they may contain. Although recently, transformer architectures have

been utilized, in addition to some convolutional ensembles for this task [2], however, YOLOv7 performs considerably in terms of precision and time-complexity.

C. Detected Text Upscaling

In most chart samples, the resolution of the text is very low resulting in poor recognition even by a mature text recognizer. Thus, we propose an additional step utilizing enhanced super resolution generative adversarial network (ESRGAN) [35] to upscale the image without losing the pixel information as compared to conventional image upscaling techniques. Image super-resolution (SR) techniques reconstruct a higher-resolution (HR) image or sequence from the observed lower-resolution (LR) images. As illustrated in Figure 5, ESRGAN is an enhanced version of super resolution GAN (SRGAN), which introduces the residual-in-residual dense block (RRDB) without batch normalization as the basic network building unit. The perceptual loss has been improved by using the features before activation, which could provide stronger supervision for brightness consistency and texture recovery. The total loss for the generator is given by Equation 5.

$$L_G = L_{\text{percep}} + \lambda L_G^{Ra} + \eta L_1, \quad (5)$$

Where L_{percep} is the perceptual loss, L_G^{Ra} is the adversarial loss for generator part in the GAN, $L_1 = \mathbb{E}_{x_i} \|G(x_i) - y\|_1$ is the content loss that evaluates the 1-norm distance between recovered image $G(x_i)$ and the ground-truth y , and λ, η are the coefficients to balance different loss terms. This proposed step helps improve the recognition accuracy in the next step significantly.

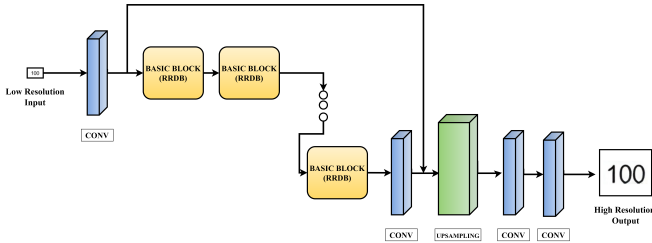


Fig. 5. Detected text upscaling. Pipeline utilizing enhanced super resolution GAN to enhance the resolution of low resolution input image that is detected text (The circled dots represent that there are more number of basic blocks)

D. Text Recognition

Text recognition is performed on the up-scaled detected text from the previous step. As the text in charts is in English, thus we have utilized a TPS-ResNet-BiLSTM-Attn [36] architecture to perform text recognition. The model applies a thin-plate spline (TPS) spatial transformation. ResNet backbone is used as a feature extractor and bi-directional long short term memory network (BiLSTM) [37] for sequence modeling. BiLSTM is a type of RNN architecture that processes input sequences in both forward and backward directions, handling variable-length input sequences and learning context from both past and future inputs making it good for sequence modeling

tasks. Finally, an additive attention mechanism is employed for the prediction part allowing the model to focus on specific parts of the input that are most relevant for making predictions.

E. Text Role Classification

Text on a chart image has a specific role. The purpose of this task is to classify the role of text. Nine roles are being considered in this study. These include chart title, mark label, legend title, legend label, axis title, tick label, tick grouping, value label, and others. It is a challenging task due to the position, orientation, and size variations of text in a chart [1], [2]. Figure 6 shows how different texts and their roles appear on a line plot. In this study, we attempt to address these challenges by fine-tuning a Swin transformer [33] as a separate classifier for text-role classification instead of using YOLOv7's recognizer. Therefore, the text detected by the YOLOv7 model is fed to the Swin transformer for role classification after upscaling. This enhances the performance of the text-role classification step in different chart types. Also Swin Transformer's ability to capture multi-scale features, positional encoding, and self-attention mechanism makes it an effective technique for handling orientation issues in chart images. We also performed experimentation using DETection TRansformer (DETR) [38] and YOLOv7. However, Swin transformer outperforms both of these techniques significantly.

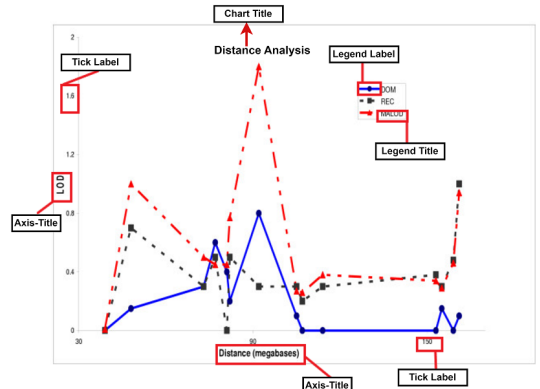


Fig. 6. An illustration of different text-roles on a line plot chart type.

III. EXPERIMENTAL PROTOCOL

This section details the experimental protocol employed in this study. The main objective of our experiments is to validate the methodology employed in each step. The scope of the study is not to propose an end-to-end system but instead provide a framework. Hence, each step is independently evaluated. In an end-to-end system, the performance of each subsequent step is dependent on the previous tasks and therefore it is hypothesized that performance improvement of one step will enhance the overall accuracy of the complete system. In the subsequent subsections, we provide details of the dataset employed followed by model training and testing for each task i.e. chart-type classification, text detection, text recognition, text enhancement, and text-role classification.

A. Dataset

To evaluate the performance of each task, we employed the ICPR2022 CHARTINFO UB PMC competition dataset [3]. The dataset provides chart images for 15 different chart types along with annotations for each image. This version of dataset has been used in ICPR 2022 challenge. It contains real charts extracted from Open-Access publications found in the PubMed Central repository. The dataset contains only real chart images, no synthetic data is included in this version. However, the number of samples for each chart type is not balanced as shown in Table II.

Moreover, for text-role classification task, we have considered only four types of charts as the data annotation for text components in these chart types is sufficient for experimental protocol as compared to other classes. The number of samples for each text-role class in these four chart types are outlined in Table I.

B. Model Training

All models are trained on a NVIDIA Tesla P100 16GB GPU hardware. 80% of the data for each task is employed for model training while 20% is used for testing purposes.

- Firstly, we train the chart-type classification model. A pre-trained Swin transformer (swin-large 224 [33]) is employed for this purpose. There are 195M trainable parameters and the train-time is 12h. The model is fine-tuned on our dataset for 50 epochs using a batch-size of 8. Adam optimizer is used with a learning rate of $lr = 0.000003$. Sparse-categorical cross-entropy loss is computed during training. We also evaluated the performance of a pre-trained ResNet150 model, but the results achieved using Swin transformers outperform those obtained by ResNet150.
- For text detection task, we applied transfer learning using a pre-trained YOLOv7 base. There are 36.9M trainable parameters and the average train-time is 16h. The model is trained for epochs: 70 (horizontal bar charts), 100 (vertical bar), 50 (line plot), and 50 (scatter plot) before convergence. A batch-size of 4 is used along with Adam optimizer at a learning rate of $lr = 0.000005$. Additional hyperparameters include a mutation scale ranging between 0-1, momentum values of 0.3, 0.6, and 0.98, and weight-decay of 1, 0.0, and 0.001.
- Output of YOLOv7 is then enhanced using a variant of enhanced super resolution generative adversarial network (ESRGAN). An upscaling of 1.5x is applied. We experimented with different upscaling values and observed that 1.5x is the optimal in most cases. Increasing this value distorted the shape of characters and affected the recognition module’s performance. Figure 7 shows a detected text from chart image, upscaling it to 1.5x improves the resolution, and upscaling to 3.0x deforms the shape of letter ‘e’.

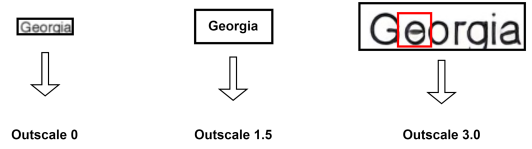


Fig. 7. Results of detected-text resolution enhancement using ESRGAN on different outscale parameter values. If the outscale parameter value is 1.5, the resolution of the input image will be enhanced to 1.5x its original resolution.

- Text recognition is performed on the output of the previous step, which is the upscaled version of detected text. For recognition purposes, we employed TPS-ResNet-BiLSTM-Attn model. The architecture utilizes a thin-plate spline transformer (TPS) to normalize the input text image. Text components in chart images usually come in diverse shapes. For recognition of such text images, a recognizer requires to learn an invariant representation with respect to geometry. To ease this process TPS employs a smooth spline transformation between a set of fiducial points. This provides flexibility of various aspect ratios. Normalized text is then mapped into feature space by a ResNet backbone. The extracted features are reshaped into a sequence and fed to a BiLSTM for modeling. An attention-based sequence prediction mechanism is then used to predict the text.
- We trained our text-role classification model, considering roles like chart-title, legend-title, legend-label, axis-title, tick-label, tick-grouping, mark-label, and value-label; using three state-of-the-art architectures: DETR [38] (100 epochs), YOLOv7 [34] (100 epochs for horizontal-bar and vertical-bar, 50 epochs for line-plot and scatter-plot), and Swin transformer (50 epochs). We employed batch sizes of 4 (YOLOv7) and 8 (Swin transformer) with respective learning rates. All models used cropped bounding box images from our dataset ground truth. Figure 8 depicts the impact of increasing epochs on classification accuracy.

C. Evaluation Metrics

For each task in the pipeline, we employ the following evaluation metrics. For chart type classification, we use Accuracy, Precision, Recall, and F1-score (given in Equation 6,7,8,9). For text detection module, we use mean Average Precision (mAP). Here mAP refers to mAP50 which is calculated by computing the average precision at only the 50% IoU threshold. For text role classification, we used F1-Score measure.

$$Accuracy = \frac{TP + TN}{TP + TN + FP + FN} \quad (6)$$

$$Precision = \frac{TP}{TP + FP} \quad (7)$$

TABLE I
DATASET DETAILS FOR TEXT-ROLE CLASSIFICATION

Chart Type	Images	mark-label	chart-title	legend-title	other	tick-grouping	axis-title	legend-label	tick-label	value-label
Horizontal Bar	787	2	83	14	733	200	647	1231	12504	3725
Vertical Bar	5454	57	118	34	1312	434	2838	3465	26441	3082
Line Plot	10556	1263	143	69	2064	38	4406	5144	32462	667
Scatter Plot	1350	589	57	52	1226	10	1832	1952	13281	55

TABLE II
DATASET DETAILS FOR CHART-TYPE CLASSIFICATION

Chart Type	No. of Images	Chart Type	No. of Images
Horizontal Bar	787	Horizontal Interval	156
Vertical Bar	5454	Manhattan	176
Line Plot	10556	Map	533
Scatter Plot	1350	Pie	242
Scatter-Line	1818	Surface	155
Vertical Box	763	Venn	75
Area	172	Vertical Interval	489
Heatmap	197	-	-

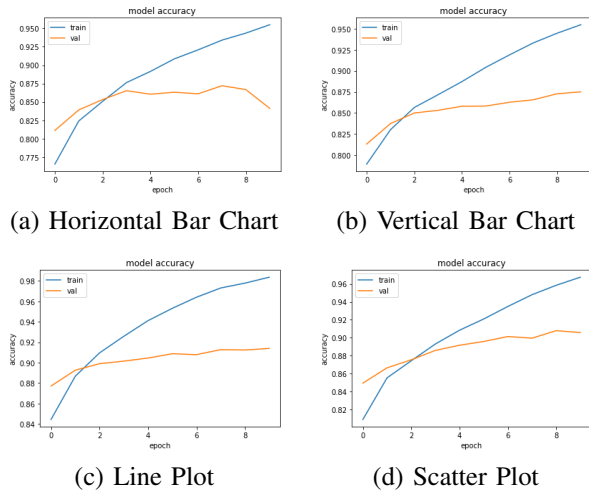


Fig. 8. Text Role Classification Train-Validation Accuracy Curves

$$Recall = \frac{TP}{TP + FN} \quad (8)$$

$$F1 = \frac{2 * Precision * Recall}{Precision + Recall} = \frac{2 * TP}{2 * TP + FP + FN} \quad (9)$$

Where TP, TN, FP, and FN are the True Positives, True Negatives, False Positives, and False Negatives, respectively.

IV. RESULTS AND DISCUSSION

In this section, we discuss the outcomes of our proposed methodologies for each task in the information extraction pipeline. Figure 9 illustrates an input chart image that is being processed through all steps of the framework pipeline.

A. Chart Type Classification Results

In chart type classification, our model achieves an F1-score of 0.97 and as it can be seen in Table III, the achieved F1-score by our model is higher than the previous techniques used for

this task such as ResNet, VGG, and Swin ensemble. Although the test set used for evaluation of these SOTA techniques was different from what we have used so direct comparison is not an option, but this reference acts as an indicator that our model performs well for this task. The model is able to correctly classify 15 chart types with an overall F1-score of 0.97 which validates that it is able to handle the style variations and other challenges mentioned earlier. The results also validate that the used hierarchical vision transformer in this task is successfully able to achieve deep position-level learning to obtain significant results.

TABLE III
PERFORMANCE COMPARISON ON CHART-TYPE CLASSIFICATION

Reference	Architecture	F1-Score
Proposed	Swin Transformer (large224)	0.970
ICDAR2019 [1]	ResNet-101	0.882
ICDAR2019 [1]	VGGNet	0.775
ICPR2020 [2]	DenseNet121+ResNet152	0.928
ICPR2020 [2]	ResNet50	0.904
ICPR2022 [3]	Swin224+Swin384	0.910

B. Text Detection and Recognition Results

For text detection, our fine-tuned YOLOv7 model is able to successfully detect text on all four chart types under consideration. The results are outlined in Table IV. The results validate that YOLOv7 in this task performs well along with other SOTA techniques utilized in recent literature.

TABLE IV
TEXT DETECTION RESULTS

Chart Type	mAP
Horizontal Bar Chart	0.953
Vertical Bar Chart	0.972
Line Plot	0.960
Scatter Plot	0.925

As mentioned earlier, due to the complex layout and variations of font styles and sizes, conventional OCRs do not perform well on chart text recognition. For this purpose, we evaluated the performance of state-of-the-art TPS-ResNet-BiLSTM-Attn model that has shown to outperform popular scene text recognition algorithms. As expected, the model is able to perform significantly better than conventional OCRs on chart text as well. However, despite its success on most text types, it did not perform well on very small-sized text as

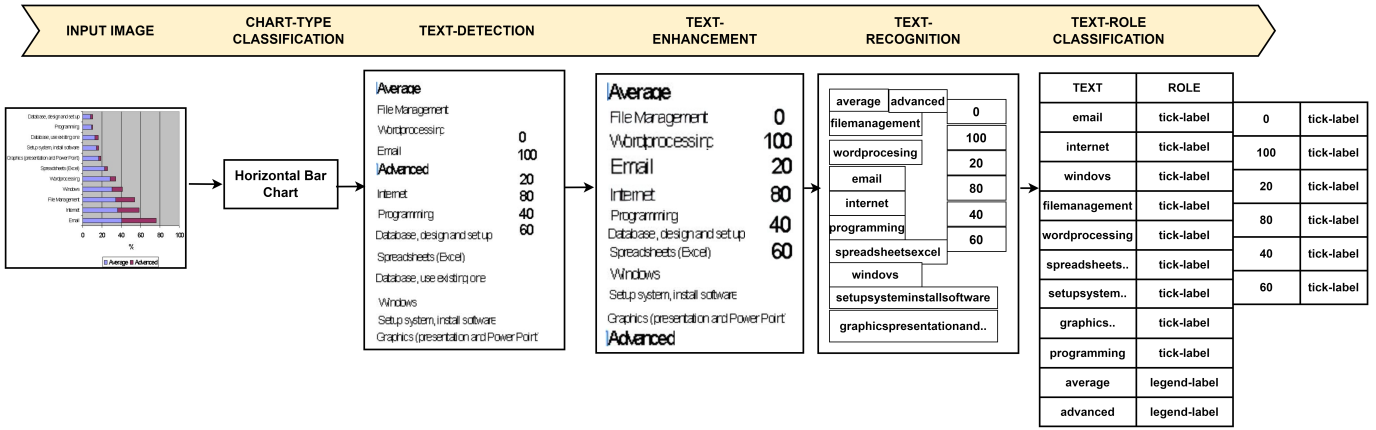


Fig. 9. An input chart image processed through all steps of the framework.

shown in Figure 10. To cater for this issue, we introduced an additional step of enhancing resolution of detected text before recognition. Figure 10 shows the improvement in recognition module after enhancement.

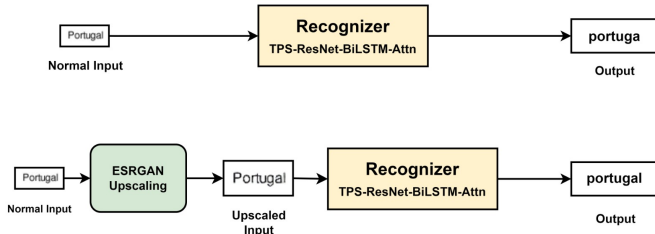


Fig. 10. Text-recognition results before & after resolution enhancement-ESRGAN.

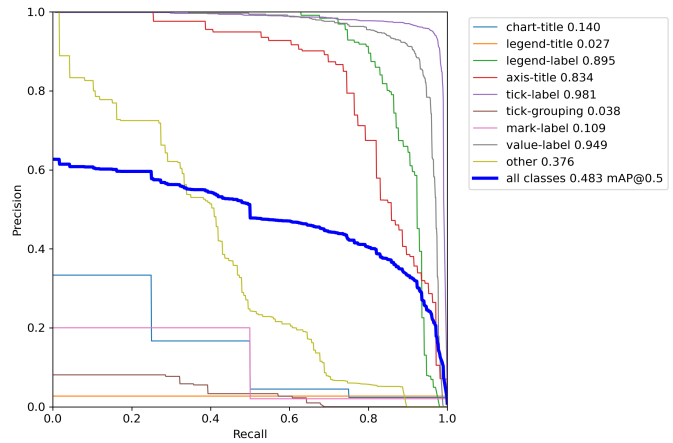


Fig. 11. YOLOv7-PR curve for text-role classification

C. Text Role Classification Results

Text style variations and relations between multiple text objects make text-role classification a challenging task for any classifier. Furthermore, placement of a specific type of text is also highly dependent on the chart type. Thus making it difficult to devise a generic tool for different types of charts. In this study, we are considering nine role classes across four different chart types. As illustrated in Table V, our trained hierarchical vision transformer using shifted windows is able to achieve considerable success in this task for all chart types. The model achieves an overall F1-Score of 0.91, 0.90, 0.86, and 0.84 for all nine text-role classes in line plot, scatter plot, vertical bar, and horizontal bar charts, respectively.

TABLE V
TEXT-ROLE CLASSIFICATION RESULTS

Chart Type	Text Role Classification			
	Accuracy	F1 Score	Precision	Recall
Horizontal Bar Chart	0.870	0.842	0.848	0.841
Vertical Bar Chart	0.875	0.866	0.866	0.875
Line Plot	0.914	0.909	0.911	0.913
Scatter Plot	0.905	0.902	0.903	0.905

V. CONCLUSION

This work marks a significant contribution to the challenging task of chart information extraction by proposing a deep learning framework for each vital step in the process. The

To understand the complexity of problem and the significance of our methodology, we compare our results with two state-of-the-art architectures YOLOv7 and DETR, where mAP is 0.40 and 0.30 from these techniques respectively. Thus, pre-trained Swin transformer fine-tuned on our data outperforms both YOLOv7 and DETR with significant margin.

Although YOLOv7 performed well in text detection but its performance in text-role classification is not satisfactory. Figure 11 shows the results of YOLOv7 for all text-role classes. Except for legend-label, axis-title, tick-label, and value-label, the model performs below satisfactory for the rest of the classes. On the other hand, Swin transformer improves overall accuracy of the text-role classification significantly.

experimentation results validate that our proposed framework performs very good, well along with other SOTA in each step with F1-scores of 0.97 and 0.91 for chart-type and text-role classification, and 0.95 mAP for text detection, respectively. We also propose a solution for low resolution small-text recognition challenge by introducing an image enhancement step using ESRGANs. The most interesting aspect of this study is the use of positional information and relational dependency between multiple objects as a supporting factor for decision making in chart-type and text-role classification by utilizing hierarchical vision transformers. Due to this, we are able to propose a generic framework for multiple chart types i.e. horizontal bar, vertical bar, line plot and scatter plot.

REFERENCES

- [1] K. Davila, B. U. Kota, S. Setlur, V. Govindaraju, C. Tensmeyer, S. Shekhar, and R. Chaudhry, "Icdar 2019 competition on harvesting raw tables from infographics (chart-infographics)," in *2019 International Conference on Document Analysis and Recognition (ICDAR)*, 2019, pp. 1594–1599.
- [2] K. Davila, C. Tensmeyer, S. Shekhar, H. Singh, S. Setlur, and V. Govindaraju, "Icpr 2020-competition on harvesting raw tables from infographics," in *International Conference on Pattern Recognition*. Springer, 2021, pp. 361–380.
- [3] K. Davila, F. Xu, S. Ahmed, D. A. Mendoza, S. Setlur, and V. Govindaraju, "Icpr 2022: Challenge on harvesting raw tables from infographics (chart-infographics)," in *2022 26th International Conference on Pattern Recognition (ICPR)*. IEEE, 2022, pp. 4995–5001.
- [4] I. Guerrini, C. C. Cook, W. Kest, A. Devitgh, A. McQuillin, D. Curtis, and H. Gurling, "Genetic linkage analysis supports the presence of two susceptibility loci for alcoholism and heavy drinking on chromosome 1p22.1-11.2 and 1q21.3-24.2," *BMC genetics*, vol. 6, no. 1, pp. 1–8, 2005.
- [5] R. O. Swai, G. R. Somi G, M. I. Matee, J. Killewo, E. F. Lyamuya, G. Kwesigabo, T. Tulli, T. K. Kabalimu, L. Ng'ang'a, R. Isingo *et al.*, "Surveillance of hiv and syphilis infections among antenatal clinic attendees in tanzania-2003/2004," *BMC Public health*, vol. 6, no. 1, pp. 1–10, 2006.
- [6] I. Baxter, P. S. Hosmani, A. Rus, B. Lahner, J. O. Borevitz, B. Muthukumar, M. V. Mickelbart, L. Schreiber, R. B. Franke, and D. E. Salt, "Root suberin forms an extracellular barrier that affects water relations and mineral nutrition in arabidopsis," *PLoS genetics*, vol. 5, no. 5, p. e1000492, 2009.
- [7] A. H. Santo, P. Puech-Leão, and M. Krutman, "Trends in aortic aneurysm-and dissection-related mortality in the state of são paulo, brazil, 1985–2009: multiple-cause-of-death analysis," *BMC Public Health*, vol. 12, pp. 1–18, 2012.
- [8] V. Karthikeyani and S. Nagarajan, "Machine learning classification algorithms to recognize chart types in portable document format (pdf) files," *International Journal of Computer Applications*, vol. 39, no. 2, pp. 1–5, 2012.
- [9] Y. P. Zhou and C. L. Tan, "Bar charts recognition using hough based syntactic segmentation," in *International Conference on Theory and Application of Diagrams*. Springer, 2000, pp. 494–497.
- [10] —, "Hough technique for bar charts detection and recognition in document images," in *Proceedings 2000 International Conference on Image Processing (Cat. No. 00CH37101)*, vol. 2. IEEE, 2000, pp. 605–608.
- [11] V. S. N. Prasad, B. Siddiquie, J. Golbeck, and L. S. Davis, "Classifying computer generated charts," in *2007 international workshop on content-based multimedia indexing*. IEEE, 2007, pp. 85–92.
- [12] Y. Zhou and C. L. Tan, "Learning-based scientific chart recognition," in *4th IAPR International workshop on graphics recognition, GREC*, vol. 7. Citeseer, 2001, pp. 482–492.
- [13] W. Huang and C. L. Tan, "A system for understanding imaged infographics and its applications," in *Proceedings of the 2007 ACM symposium on Document engineering*, 2007, pp. 9–18.
- [14] S. R. Choudhury, S. Wang, and C. L. Giles, "Scalable algorithms for scholarly figure mining and semantics," in *Proceedings of the International Workshop on Semantic Big Data*, 2016, pp. 1–6.
- [15] M. Savva, N. Kong, A. Chhajta, L. Fei-Fei, M. Agrawala, and J. Heer, "Revision: Automated classification, analysis and redesign of chart images," in *Proceedings of the 24th annual ACM symposium on User interface software and technology*, 2011, pp. 393–402.
- [16] S. Shukla and A. Samal, "Recognition and quality assessment of data charts in mixed-mode documents," *International Journal of Document Analysis and Recognition (IJDAR)*, vol. 11, no. 3, pp. 111–126, 2008.
- [17] B. Tang, X. Liu, J. Lei, M. Song, D. Tao, S. Sun, and F. Dong, "Deepchart: Combining deep convolutional networks and deep belief networks in chart classification," *Signal Processing*, vol. 124, pp. 156–161, 2016.
- [18] S. C. Daggubati, J. Sreevalsan-Nair, and K. Dadhich, "Barchartanalyzer: Data extraction and summarization of bar charts from images," *SN Computer Science*, vol. 3, no. 6, pp. 1–19, 2022.
- [19] J. Choi, S. Jung, D. G. Park, J. Choo, and N. Elmqvist, "Visualizing for the non-visual: Enabling the visually impaired to use visualization," in *Computer Graphics Forum*, vol. 38, no. 3. Wiley Online Library, 2019, pp. 249–260.
- [20] W. Dai, M. Wang, Z. Niu, and J. Zhang, "Chart decoder: Generating textual and numeric information from chart images automatically," *Journal of Visual Languages & Computing*, vol. 48, pp. 101–109, 2018.
- [21] R. A. Al-Zaidy and C. L. Giles, "Automatic extraction of data from bar charts," in *Proceedings of the 8th international conference on knowledge capture*, 2015, pp. 1–4.
- [22] J. POCO and J. Heer, "Reverse-engineering visualizations: Recovering visual encodings from chart images," in *Computer graphics forum*, vol. 36, no. 3. Wiley Online Library, 2017, pp. 353–363.
- [23] J. POCO, A. Mayhua, and J. Heer, "Extracting and retargeting color mappings from bitmap images of visualizations," *IEEE transactions on visualization and computer graphics*, vol. 24, no. 1, pp. 637–646, 2017.
- [24] K. He, G. Gkioxari, P. Dollár, and R. Girshick, "Mask r-cnn," in *Proceedings of the IEEE international conference on computer vision*, 2017, pp. 2961–2969.
- [25] X. Liu, D. Klabjan, and P. NBless, "Data extraction from charts via single deep neural network," *arXiv preprint arXiv:1906.11906*, 2019.
- [26] Z. Cai and N. Vasconcelos, "Cascade r-cnn: high quality object detection and instance segmentation," *IEEE transactions on pattern analysis and machine intelligence*, vol. 43, no. 5, pp. 1483–1498, 2019.
- [27] X. Qin, Y. Zhou, Y. Guo, D. Wu, Z. Tian, N. Jiang, H. Wang, and W. Wang, "Mask is all you need: Rethinking mask r-cnn for dense and arbitrary-shaped scene text detection," in *Proceedings of the 29th ACM International Conference on Multimedia*, 2021, pp. 414–423.
- [28] R. Smith, "An overview of the tesseract ocr engine," in *Ninth international conference on document analysis and recognition (ICDAR 2007)*, vol. 2. IEEE, 2007, pp. 629–633.
- [29] R. Al-Zaidy and C. Giles, "A machine learning approach for semantic structuring of scientific charts in scholarly documents," in *Proceedings of the AAAI Conference on Artificial Intelligence*, vol. 31, no. 2, 2017, pp. 4644–4649.
- [30] C. Wang, K. Cui, S. Zhang, and C. Xu, "Visual and textual information fusion method for chart recognition," in *International Conference on Pattern Recognition*. Springer, 2021, pp. 381–389.
- [31] Y. Xu, M. Li, L. Cui, S. Huang, F. Wei, and M. Zhou, "Layoutlm: Pre-training of text and layout for document image understanding," in *Proceedings of the 26th ACM SIGKDD International Conference on Knowledge Discovery & Data Mining*, 2020, pp. 1192–1200.
- [32] Z. Luo, Z. Zhang, G. Li, L. Che, J. He, and Z. Xu, "A benchmark for analyzing chart images," in *International Conference on Pattern Recognition*. Springer, 2021, pp. 390–400.
- [33] Z. Liu, Y. Lin, Y. Cao, H. Hu, Y. Wei, Z. Zhang, S. Lin, and B. Guo, "Swin transformer: Hierarchical vision transformer using shifted windows," *CoRR*, vol. abs/2103.14030, 2021. [Online]. Available: <https://arxiv.org/abs/2103.14030>
- [34] C.-Y. Wang, A. Bochkovskiy, and H.-Y. M. Liao, "Yolov7: Trainable bag-of-freebies sets new state-of-the-art for real-time object detectors," *arXiv preprint arXiv:2207.02696*, 2022.
- [35] X. Wang, K. Yu, S. Wu, J. Gu, Y. Liu, C. Dong, C. C. Loy, Y. Qiao, and X. Tang, "ESRGAN: enhanced super-resolution generative adversarial networks," *CoRR*, vol. abs/1809.00219, 2018. [Online]. Available: <http://arxiv.org/abs/1809.00219>
- [36] J. Baek, G. Kim, J. Lee, S. Park, D. Han, S. Yun, S. J. Oh, and H. Lee, "What is wrong with scene text recognition model comparisons? dataset and model analysis," *CoRR*, vol. abs/1904.01906, 2019. [Online]. Available: <http://arxiv.org/abs/1904.01906>

- [37] Z. Huang, W. Xu, and K. Yu, "Bidirectional LSTM-CRF models for sequence tagging," *CoRR*, vol. abs/1508.01991, 2015. [Online]. Available: <http://arxiv.org/abs/1508.01991>
- [38] N. Carion, F. Massa, G. Synnaeve, N. Usunier, A. Kirillov, and S. Zagoruyko, "End-to-end object detection with transformers," *CoRR*, vol. abs/2005.12872, 2020. [Online]. Available: <https://arxiv.org/abs/2005.12872>